Incorporating observed nighttime conductance alters global hydrology and carbon budgets in CLM4.5.

Lombardozzi, D.L.[1*], Zeppel, M.J.B [2], Fisher, R.A[1]. Tawfik, A.[1,3]

[1]National Center for Atmospheric Research, Boulder, CO, USA

[2]Department of Biological Sciences,
Macquarie University, Sydney, Australia.

[3]Center for Ocean-Land-Atmosphere Studies
George Mason University, Fairfax, VA, USA

[*] Corresponding author email: dll@ucar.edu

16 **Abstract**

17 The terrestrial biosphere regulates climate through carbon, water, and
18 energy exchanges with the atmosphere. Land surface models estimate plant
19 transpiration, which is actively regulated by stomatal pores, and provide
20 projections essential for understanding Earth's carbon and water resources.
21 Empirical evidence from 204 species suggests that significant amounts of water
22 are lost through leaves at night, though land surface models typically reduce
23 stomatal conductance to nearly zero at night. Here, we test three different
24 methods of incorporating observed nighttime stomatal conductance values to a
25 global land surface model, the Community Land Model (CLM) version 4.5, to
26 better constrain carbon and water budgets. We find that our modifications
27 increase transpiration up to 5% globally, reduce modeled available soil moisture
28 by up to 50% in semi-arid regions, and increase the importance of the land
29 surface in modulating energy fluxes. Carbon gain declines up to ~4% globally
30 and >25% in semi-arid regions. We advocate for realistic constraints of
31 minimum stomatal conductance in future climate simulations, and widespread
32 field observations to improve parameterizations.

33

34 **1. Introduction**

35 Terrestrial plants must balance their need to obtain CO_2 with the risk of
36 desiccation if transpiration continues unchecked. Higher plants evolved stomatal
37 pores to control the exchange of water and carbon between the leaf interior and
38 the atmosphere (Hetherington and Woodward, 2003). Stomatal function, thus, is
39 the dominant control over terrestrial fluxes of water and carbon. Most large-
40 scale land-surface models use an empirical representation of stomatal

conductance (g_s), similar to the Ball-Woodrow-Berry (BWB) model (Ball, 1988; Ball et al., 1987; Collatz et al., 1991; Leuning, 1995; Medlyn et al., 2011; Sellers et al., 1996), to calculate plant gas exchange. The BWB model is linear, with two constants, the intercept (g_o) and slope (g_1), and estimates g_s from the rate of CO_2 assimilation (A), atmospheric humidity (h_r), and internal leaf CO_2 concentration. The original BWB model parameters were fitted to observations of leaf gas exchange for ten plant species, with different g_o values for each species, ranging from -310 to 130 mmol m^{-2} s^{-1} (Ball, 1988). The Community Land Model (CLM), however, uses only two g_o values, (10 and 40 mmol m^{-2} s^{-1} for C_3 plants and C_4 plants, respectively; Collatz et al., 1991; Oleson et al., 2013; Sellers et al., 1996). Conductance during the night (and at other times when A is 0) is thus represented using g_o. Recent advances in our ability to observe nighttime stomatal conductance (Caird et al., 2007; Phillips et al., 2010), $g_{s,n}$, illustrate that values are often larger in the field than the BWB parameters used in the CLM.

A comprehensive database (see Table S1) of 204 observed $g_{s,n}$ values illustrates that the minimum BWB g_s values (equivalent to g_o) used in the CLM starkly differ with observed mean and median $g_{s,n}$ values. The available data for $g_{s,n}$ range from 0-450 mmol m^{-2} s^{-1} with an overall mean of 78 mmol m^{-2} s^{-1} (excluding hemi-parasites and CAM plants, which were omitted from model testing). Observations of $g_{s,n}$ are, on average, ten times higher in broadleaf tropical deciduous species (Table 1; 129 mmol m^{-2} s^{-1}) and seven times higher in temperate broadleaf deciduous trees (73 mmol m^{-2} s^{-1}) compared to the 10 mmol m^{-2} s^{-1} used for C_3 plants. Potential benefits of a high $g_{s,n}$ might include the transport of nutrients (Dios et al., 2013; Scholz et al., 2007; Zeppel et al., 2014) or processes related to embolism repair, phloem transport, or xylem refilling that

might improve carbon gain, but these ideas remain untested. Nonetheless, the discrepancy between parameterized g_o and observed $g_{s,n}$ serves as motivation to investigate the sensitivity of simulated land surface processes to more realistic minimum g_s values. Such field measurements of $g_{s,n}$ have not previously been incorporated into a global land surface model, despite the possible impacts on surface hydrology, ecosystem carbon gain, and land-atmosphere feedbacks.

We use a global land-surface model, the Community Land Model (CLM) version 4.5, forced with a data atmosphere and driven with observed ('satellite phenology') leaf area indices (CLM4.5SP), to test the sensitivity of the land surface to using realistic minimum g_s from observed $g_{s,n}$, averaged by plant functional type (PFT; Table 1). Since the BWB approach is primarily intended to predict daytime stomatal behavior, the appropriate method for application of observed $g_{s,n}$ within the context of the BWB model is unclear. We therefore test three methodologies for implementing observed $g_{s,n}$: 1) modifying the BWB intercept (g_o); 2) setting a nighttime threshold value; and 3) setting a minimum threshold value. We anticipate that implementing observed $g_{s,n}$ values will increase plant transpiration, altering carbon and water budgets on regional and global scales.

2. Methods

2.1 Modeling

The CLM4.5SP model used here is an updated version of CLM4.0, originally described by Lawrence et al., (2011), with updated technical details for v4.5 described by Oleson et al., (2013). The CLM4.5SP simulations were run with

CRU-NCEP climate forcing data (combines Climate Research Unit (CRU) TS 3.2 monthly climatology with National Oceanic and Atmospheric Administration National Center for Environmental Prediction (NCEP) and NCAR 2.5° x 2.5° 6-hourly reanalysis; (downloaded at: http://dods.ipsl.jussieu.fr/igcmg/IGCM/BC/OOL/OL/CRU-NCEP/), a historical atmospheric dataset that includes observed precipitation, temperature, downward solar radiation, surface wind speed, specific humidity, and air pressure from 1901 through 2010, and did not include the influences of nitrogen deposition, land use change, or changing CO_2 concentrations.

The CLM4.5SP uses the coupled Farquhar photosynthesis and BWB g_s models to simulate plant physiology (Bonan et al., 2011; Oleson et al., 2013). The BWB g_s is calculated based on the equation:

$$g_s = g_0 + g_1(Ah_r/C_a) \qquad (Eq.\ 1)$$

where g_0 and g_1 are empirical fitting parameters of the minimum g_s and the slope of the conductance-photosynthesis relationship, respectively; A is net carbon assimilation rate (μmol C m^{-2} s^{-1}); h_r is the fractional humidity at the leaf surface (dimensionless), and C_a is the CO_2 concentration at the leaf surface (μmol mol^{-1}). When implemented in the unmodified CLM4.5SP, g_0 is 10 mmol m^{-2} s^{-1} for all C_3 plants and 40 mmol m^{-2} s^{-1} for all C_4 plants, and is adjusted by a soil wetness factor (varying from 0-1) every time-step.

Values of $g_{s,n}$ based on literature data (Table S1) are typically larger than the g_0 values used in current implementations of the BWB model. The $g_{s,n}$ data, grouped and then averaged by PFT (Table 1), were used to modify simulated minimum g_s using three methodologies. First, the 'Δg_0' method replaced the BWB minimum conductance, g_0, value for each simulated PFT with the observed $g_{s,n}$

(Table 1), resulting in a uniform increase to g_s during both day and night (referred to as the Δg_o simulation; tested previously by Barnard and Bauerle, 2013). Second, the Δg_{night} method implemented the BWB model in its standard form (Eq. 1; the g_o and g_1 values are the same as the control), but included a minimum threshold that was applied only at night, based on observed $g_{s,n}$ for each PFT, below which g_s could not fall. In the Δg_{night} simulation, daytime Δg_s occasionally fell below the observed nighttime threshold on account of high vapor pressure deficit (VPD) or low assimilation rates. To avoid this potentially unrealistic behavior, we use a third method, 'Δg_{min}', which extended the observation-based threshold used in the Δg_{night} simulation to all times during the day or night, so that g_s never fell below the minimum threshold value found in Table 1. These three modified simulations were compared to a control simulation using the unmodified BWB formulation. Similar to the unmodified simulation that adjusts the g_o parameter based on a soil wetness scalar (β_{soil}), the Δg_{night} and Δg_{min} modifications also adjusted the minimum g_s threshold by a soil wetness scalar, β_{soil}, that ranges from zero to one, at every time-step. Each simulation was run for 25 years with monthly output to determine the long-term impact of changing minimum conductance, and for one year with half-hourly output to determine the changes in diel patterns.

2.2 Data Collection

Values of $g_{s,n}$ were obtained from field and glasshouse studies, using Scopus (www.scopus.com), with data for 204 records across 150 species and cultivars (Table S1). Records available were predominately for temperate plants (93 records) and crops (34), with more data available for broad-leaf plant types

141 (89) than needle-leaf plants (16; Zeppel et al., 2014). The data were collated by
142 plant functional type (PFT), with means, medians, and standard deviations for
143 each PFT presented in Table 1. Simulations presented here were run with mean
144 values for each PFT, though median values were also tested and are presented in
145 SI Figure 3 and SI Figure 4. Since there is large variability in the PFT responses,
146 we present the range of variability in SI Figure 2.
147 The measurements of each $g_{s,n}$ value are generally obtained from steady
148 state porometers, diffusion porometers, Licor 1600 and Licor 6400 gas exchange
149 systems (Caird et al., 2007; Phillips et al., 2010), with a small number converted
150 from sap flux (Benyon 1999) using an inverted Penman-Monteith equation.
151 Different sampling methods may lead to different estimates of $g_{s,n}$, and
152 measureable $g_{s,n}$ typically only occurs where VPD is above zero. For example,
153 using a cuvette clamped over the leaf, which changes the leaf boundary layers,
154 will be different compared to measurements from sap flow with an unaltered
155 boundary layer. Data for $g_{s,n}$ were typically reported during well-watered
156 conditions, which is ideal because the CLM4.5 calculates stomatal g_s without
157 water stress and then adjusts g_o values (and modifications additionally adjust
158 g_{night} and g_{min} thresholds) using a soil wetness scalar.
159
160 *2.3 Terrestrial Coupling Index*
161 To investigate the impact of stomatal conductance changes on the degree
162 to which land processes exert influence over the atmosphere, a terrestrial
163 coupling index was calculated, allowing examination of the influence of a
164 minimum g_s threshold on land-atmosphere coupling. Following Dirmeyer
165 (2011), the terrestrial segment of land-atmosphere coupling is defined as:

166

167 $$\text{Terrestrial Coupling Index (TCI)} = \sigma_w * \beta_{w,ET} \quad \textit{(Eq. 2)}$$

168

169 where σ_w is the standard deviation of root-zone soil moisture relevant for
170 transpiration across a given season (e.g., 25 years times 3 summer months), and
171 $\beta_{w,ET}$ is the linear slope of monthly mean evapotranspiration and root-zone soil
172 moisture. The TCI captures the variability (σ_w) and sensitivity of
173 evapotranspiration to changes in soil moisture and returns units equivalent to
174 those of evapotranspiration. Therefore, for a region to have high TCI, soil
175 moisture must have high variability thus enabling any evapotranspiration-soil
176 moisture sensitivity to manifest in the climate system. While this is strictly a
177 metric for defining the terrestrial component of coupling, the terrestrial
178 component has been used as a surrogate for the total soil moisture-precipitation
179 coupling pattern because of the strong spatial pattern correlation (Wei and
180 Dirmeyer, 2012).

181

182 **3. Results and Discussion**

183 *3.1 Implementation of $g_{s,n}$*

184 Incorporating observed minimum constraints on g_s in all modified
185 simulations increased g_s and transpiration compared to the control simulation,
186 illustrated in Fig. 1 for a highly impacted semi-arid location in Ethiopia (see Fig.
187 S1 for other regions). The large variability in the observational dataset causes
188 substantial uncertainty in the simulations, masking the differences among
189 parameterizations and highlighting the impact of $g_{s,n}$ on transpiration (Fig. S2).
190 The sensitivity of g_s and transpiration to the altered g_o parameter in the Δg_o

191 simulation is large (Barnard and Bauerle, 2013; Bowden and Bauerle, 2008).
192 Since the higher g_o is added to g_s in the BWB calculation at every model time step
193 (see Eq. 1), altering g_o increases transpiration throughout the entire diel cycle,
194 and produces changes in the daytime evaporative flux that are not supported by
195 observations of $g_{s,n}$. We consider that uniformly adjusting the g_o parameter does
196 not represent the correct implementation of observed $g_{s,n}$ values.
197 If g_o cannot be equated to plant minimum g_s in the BWB paradigm, this
198 raises the possibility of whether g_o has a theoretical interpretation beyond an
199 empirical fitting parameter. It is possible that g_o is equivalent to cuticular
200 conductance (g_{cut}), or conductance that is not regulated by the stomatal guard
201 cells (Caird et al., 2007), occurring during the day and night. Niyogi and Raman
202 (1997) describe g_o as cuticular conductance, though there is no record of g_o
203 being tested or described as g_{cut} previously. Studies that have quantified g_{cut}
204 found that g_{cut} was a low proportion, < 10%, of total g_s and less than measured
205 $g_{s,n}$ (Caird et al., 2007; Zeppel et al., 2014). The values of g_o used in current
206 implementations of the Ball-Berry model for C_3 plants (10 mmol m^{-2} s^{-1}) fall
207 within the range of measured g_{cut} values (4 to 20 mmol m^{-2} s^{-1}; Caird et al., 2007).
208 Assuming g_o does have a theoretical function of representing g_{cut}, rather than $g_{s,n}$,
209 incorporating an observed threshold of minimum g_s is necessary. Whether g_o
210 functions theoretically as g_{cut} in the BWB model needs further evaluation, as
211 adjusting simulated g_o has large impacts on canopy conductance and
212 transpiration (Fig 1; Barnard and Bauerle, 2013). Regardless, observed $g_{s,n}$ is
213 larger than modeled g_o and functions differently, and therefore should be
214 considered independently in model parameterizations.

215 The Δg_{min} and Δg_{night} simulations represent the intended change in
216 minimum g_s with greater fidelity, by limiting the minimum value without
217 increasing g_s at every model time step. Interestingly, in restricting only
218 nighttime conductance, the Δg_{night} simulation allows daytime g_s to decrease
219 below the nighttime threshold during the dry season in semi-arid ecosystems
220 (Fig. 1a). This occurs when A_n nears zero in shade or low humidity, causing g_s to
221 fall to the default (lower) g_o. In contrast, the Δg_{min} simulation restricts minimum
222 g_s at all times, and therefore daytime values are never less than the water-
223 adjusted $g_{s,n}$. This increases canopy-averaged daytime g_s, and hence
224 transpiration, compared to the unmodified simulation whenever daytime g_s
225 values fall below the minimum threshold (Fig. 1a, c).
226 The data in Table S1 is a compilation of all available published $g_{s,n}$ data to
227 date, and reports $g_{s,n}$ values for 204 distinct plants. Of these, only four plants
228 exhibit higher $g_{s,n}$ than daytime g_s, and two of those are Crassulacean acid
229 metabolism (CAM) plants, which by definition open their stomata at night to gain
230 carbon dioxide and close their stomata during the day, and were not used in our
231 parameterization. These data suggest that, as expected, $g_{s,n}$ is typically less than
232 daytime g_s. Most data presented in Table S1 are average values under non-
233 drought stressed conditions, and are likely only reported for leaves in sunlit
234 canopy layers. Thus, these data do not elucidate whether, at any given time,
235 daytime values might drop below the nighttime threshold, but only suggest that,
236 on average, they do not.

237 In the context of the model simulations, low daytime g_s occurs any time
238 that Ah_r/C is low. These are conditions which are poorly illuminated (in shade or

239 at dawn/dusk and night), or when humidity is low. The CLM4.5SP contains a
240 representation of the shaded canopy, which has lower g_s and often reaches the
241 minimum daytime threshold (g_o in the unmodified, Δg_o, and Δg_{night} simulations;
242 and $g_{s,n}$ in the Δg_{min} simulation). The central issue in determining whether the
243 Δg_{min} or Δg_{night} simulation is a better representation of minimum g_s is whether,
244 under the same conditions in the real world, daytime g_s might be lower than $g_{s,n}$.
245 For example, if observational data support that daytime g_s is less than $g_{s,n}$ in
246 shaded canopy layers, then the Δg_{night} simulation is a better parameterization.
247 However, if observational data suggest that daytime g_s is consistently higher
248 than $g_{s,n}$, then the Δg_{min} simulation is a better parameterization. While
249 observational data are not available to specifically answer this question, the
250 available data (presented in Table S1) imply that daytime g_s is on average higher
251 than $g_{s,n}$, providing partial support for the Δg_{min} implementation.

252 The possible existence of a higher $g_{s,n}$ compared to daytime g_s raises an
253 interesting question about the potential selective advantage for leaves with a
254 high $g_{s,n}$. It is hypothesized that high $g_{s,n}$ may provide a beneficial function to the
255 plant, such as embolism repair or phloem transport. Additionally, $g_{s,n}$ may
256 contribute to xylem refilling, potentially improving carbon gain by making water
257 available when light conditions allow for photosynthesis. Critically, it is not clear
258 whether these potential functions are only relevant at night (and daytime g_s can
259 be lower than $g_{s,n}$), or whether high $g_{s,n}$ is representative of a general strategy of
260 higher overall minimum g_s. We are not aware of data that exist to support either
261 possibility, and advocate for observations that will help determine the functional
262 significance of $g_{s,n}$.

From a model or theoretical perspective, it is important to note that the reason that simulated g_s values are reduced to as low as 10 mmol m^{-2} s^{-1} (or lower, if down-regulated for water stress) is a function of the universal parameterization of all C_3 plants with that value of g_o. Given that it is unlikely that this value is universal for all plants, we consider that the large difference between the Δg_{min} or Δg_{night} simulations is an artifact of the poorly constrained parameterization of the daytime BWB model.

It should be noted that all the minimum thresholds implemented in our simulations (Δg_o, Δg_{night}, and Δg_{min}) are adjusted by a soil water scalar (β_{soil}). Therefore, the nighttime (Δg_{night}) and the minimum (Δg_{min}) thresholds are altered according to the degree of soil moisture stress. When the daytime g_s value is lower than the g_{night} threshold in the Δg_{night} simulation (Fig. 1c), the g_{night} threshold is already down-regulated for water stress. In this scenario, the daytime minimum g_s is less than the nighttime g_s when water stress is equivalent.

Responses to dry soil conditions are mediated both through the minimum g_s values, and through the impact of soil moisture on photosynthetic capacity and leaf maintenance respiration, which are also multiplied by $\beta_{soil.}$ Many of the impacts of our simulations result from feedbacks between higher transpiration rates resulting in faster depletion of soil moisture store, and therefore greater constraint on photosynthesis. These results are all emergent features of the model and should not be interpreted as direct results of the altered parameterization.

3.2 Global Water and Carbon

When averaged over 25 years, incorporating observed rates of $g_{s,n}$ in the Δg_{min} simulation increased transpiration losses up to 30% in the Amazon, and >30% in some arid regions, in part due to the small absolute magnitude of available soil water (Fig. 2a-c). Semi-arid regions are primarily broad-leaf shrub and C_3 grass PFTs that have particularly high values (130 and 156 mmol m^{-2} s^{-1} respectively) of observed $g_{s,n}$ (Table 1), and have high nighttime vapor pressure deficits that interact with higher minimum g_s values, causing large nighttime transpiration rates. Using median rather than mean values caused only small (<1.5%) differences in global transpiration (Fig. S3, Fig. S4). Though the magnitude of response is different depending on parameterization used, the increases in transpiration imply that current model estimates of plant water loss are underestimated in many regions.

Simulated higher transpiration resulting from higher minimum g_s also has ecosystem-scale ramifications for hydrology (McLaughlin et al., 2007). For example, the increased transpiration resulted in drier soils compared to the control simulation (Fig. 2g-i), with Δg_{min} causing >40% soil moisture decreases in semi-arid ecosystems like the Southwestern United States and much of Australia (>10% in Δg_{night}). Additionally, the Δg_{min} estimated changes to surface runoff are large in some regions, such as the 10-25% decreases in the tropics (5-10% in Δg_{night}; Fig. 2d-f), suggesting that current runoff estimates may be too large. It should be noted that the difference between the Δg_{min} and Δg_{night} simulations is largely due to changes in minimum g_s that affect daytime g_s (see Section 3.1). Hydrologic changes in soil moisture and runoff in response to increased g_s have previously been documented in catchments in southeastern United States (McLaughlin et al., 2007), and our results suggest that changes to stomatal

conductance have similar consequences in CLM4.5SP simulations. Additionally, increasing minimum g_s caused gross primary productivity (GPP) to decrease (Figure 3) by 10 to >25% in many semi-arid regions. These are regions where water availability already restricts GPP, and the decreases in soil moisture caused by higher transpiration likely impart even more drought-induced stomatal closure.

To more directly evaluate the potential influence of minimum g_s on the climate system, we calculate the change in terrestrial coupling to the atmosphere. The terrestrial coupling index (Dirmeyer, 2011) estimates the degree to which changes in soil moisture control surface energy fluxes to the atmosphere. This study uses root-zone soil moisture rather than soil moisture over spatially constant soil depth to highlight the direct impact of vegetation and minimum g_s on surface fluxes. Here we calculate the terrestrial coupling index during boreal summer months when warmer temperatures allow for the highest g_s rates. We find that the terrestrial coupling strength increases when using the Δg_{min} implementation, but is generally unchanged for Δg_{night} (Fig. 4), meaning root-zone soil moisture exerts a greater control on surface flux variability for Δg_{min}, largely due to the impact this simulation has on daytime g_s. This increased terrestrial coupling to the atmosphere largely mirrors the reductions in GPP and soil moisture in semi-arid ecosystems, and may reinforce climate extremes such as droughts or heat waves (Hirschi et al., 2011; Miralles et al., 2014).

3.3 Evaluating $g_{s,n}$

Evaluating the performance of the new $g_{s,n}$ parameterizations is challenging for numerous reasons. First, our model scales from leaf-level g_s and $g_{s,n}$ estimates to canopy transpiration. The best way of evaluating the model is to

337 compare simulated and observed canopy transpiration because the model
338 captures the average of an entire canopy, which is comprised of multiple plant
339 functional types, rather than individual plant functional types. Incorporating
340 realistic minimum g_s increases global evapotranspiration and decreases global
341 runoff compared to globally-scaled observations, while estimates of GPP from all
342 simulations fall within the range of global GPP estimates from observations
343 (Table 2; Bonan et al., 2011, 2012; Li et al., 2011). However, these comparisons
344 should be used with caution, since eddy covariance data used in estimating the
345 GPP and evapotranspiration observations are susceptible to errors at night
346 (Fisher et al., 2007; van Gorsel et al., 2008; Kirschbaum et al., 2007; Medlyn et al.,
347 2005) due to a lack of sufficient canopy turbulence that precludes detection of
348 nighttime transpiration using this measurement methodology, and are not useful
349 for evaluating the changes in water fluxes tested in this study. Other data for
350 evaluating model responses to minimum g_s on large spatial scales are not yet
351 available.

352 A comparison of simulated canopy transpiration to transpiration
353 calculated from sap-flux data in Australia (Fig. 5) illustrates that a minimum g_s
354 threshold changes transpiration estimates during the early part of the night,
355 though simulated nighttime rates are still low compared to observations. All
356 model parameterizations fall within the observational range of uncertainty, but
357 under-predict nighttime and midday canopy transpiration during May and June,
358 and over-predict midday canopy transpiration in July. The lack of fidelity
359 between the various model parameterizations and the observations is likely
360 affected by the fact that observed meteorological data were unavailable to force
361 the model. Therefore, key parameters driving both daytime and nighttime

362 transpiration fluxes, such as VPD and soil water availability, were likely different
363 in the model simulations compared to the actual meteorological conditions at
364 Castlereagh during data collection. Additionally, because sap flow is measured at
365 the base of the tree, there is typically a lag between when sap flow is measured
366 and when the canopy transpires, and this lag is also notable in comparing
367 observed sap flow with simulated estimates of transpiration. Estimating
368 nighttime transpiration using sap flow methodology is also convoluted with the
369 refilling of aboveground water stores depleted during the day, and thus is not
370 directly comparable to our simulations. It should also be noted that the model
371 does not have a semi-arid plant functional type, so semi-arid plants are typically
372 represented in the model as deciduous plant functional types.

373 Given that our study focused only on one aspect of the g_s formulation
374 within a land surface model, evaluating daytime g_s and other aspects of the BWB
375 model function (i.e., photosynthetic drivers of daytime g_s, feedbacks to water
376 availability, etc.) are all subject to pre-existing deficiencies in the representation
377 of a host of other model processes. For example, there are only two values of the
378 g_1 (slope) parameter in the BWB model, one for C_3 and one for C_4 plants (Sellers
379 et al., 1996), and this parameter has not been modified or comprehensively
380 evaluated within the context of the CLM4.5SP. Indeed, the use of the BWB model
381 at all is currently the subject of some debate (Bonan et al., 2014; De Kauwe et al.,
382 2015). Further, daytime g_s is also dependent on the photosynthetic capacity, and
383 observations of V_{cmax} and J_{max} (Bonan et al., 2011; Kattge and Knorr, 2007)
384 indicate very wide ranges of plant functional type variation in these properties,
385 also limiting our confidence that the globally averaged parameters used in the
386 default model will lead to accurate g_s and transpiration at most locations. We

choose not to focus on these and other parameters that effect daytime g_s, as it does not directly impact the representation of $g_{s,n}$, and is therefore beyond the scope of this paper.

4. Conclusion

The rate of minimum g_s estimated from the BWB model used in many global land surface models is typically smaller than observed $g_{s,n}$ (Barnard and Bauerle, 2013), as demonstrated in a review of 204 species (Zeppel et al., 2014). Including a nighttime or minimum g_s threshold based on observations results in simulated hydrologic changes, such as decreased soil moisture and runoff (Fig. 2), particularly in semi-arid regions where water availability already restricts growth. In addition to potentially increasing drought stress in sensitive regions, this has the impact of reducing plant growth (Fig. 3) and changing the modeled terrestrial coupling to the atmosphere (Fig. 4). The difference between the Δg_{min} and Δg_{night} simulations highlights one outstanding uncertainty: Does minimum daytime g_s decrease below nighttime g_s? While the balance of our arguments favors the Δg_{min} implementation of $g_{s,n}$, this study primarily illustrates the potential sensitivity of global simulations to minimum g_s considerations, and serves as motivation for additional field experiments, particularly in semi-arid areas, to discern better representations of low g_s conditions during daytime and nighttime. To better understand the future of these sensitive ecosystems, widespread field observations, quantification of minimum daytime g_s, and a better understanding of the physiological causes and consequences of nighttime transpiration are necessary so that land surface models can robustly incorporate observations and theory.

5. Code and Data Availability

The code for CLM4.5 is publically available through Subversion code repository: https://svn-ccsm-models.cgd.ucar.edu/cesm1/release_tags/cesm1_2_2. To access the code, fill out a short, required registration to get a user name and password, necessary to gain access to the repository. http://www.cesm.ucar.edu/models/register/register_cesm.cgihttp://www.cesm.ucar.edu/models/cesm1.2/clm/CLM45_Tech_Note.pdf. The CLM4.5 User's Guide can be found at: http://www.cesm.ucar.edu/models/cesm1.2/clm/models/lnd/clm/doc/UsersGuide/book1.html. All stomatal conductance data used in developing the implementations can be found in Table S1.

Author Contributions

DL, MZ, and RF conceived the project. MZ assembled the $g_{s,n}$ datasets; DL ran model simulations; and DL and AT analyzed model simulations, with guidance from RF. All authors contributed to writing the paper.

Acknowledgements

We thank Gordon Bonan for useful discussion on the manuscript, and the reviewers for the constructive comments that have improved the final version of this paper. DL was supported through the DEB-Ecosystem Science cluster and National Science Foundations grant EF-1048481. MZ was supported by ARC DECRA DE120100518. RF was supported by the National Science Foundation and the National Center for Atmospheric Research, and AT was supported by the National Science Foundation grant 0947837 for Earth System Modeling post-

437 doctoral fellows. The National Center for Atmospheric Research is funded by the
438 National Science Foundation.

Tables

Table 1. Old and new minimum stomatal conductance values used in CLM4.5SP. Units are mmol m^{-2} s^{-1}

Plant Functional Type	Old Value	Mean New Value	Median New Value	Standard Deviation	n
temperate needle-leaf evergreen tree	10	16.896	10	20.80332642	12
boreal needle-leaf evergreen tree	10	8	8	NA	1
needle-leaf deciduous tree	10	35.367	35	6.457811807	3
tropical broadleaf evergreen tree	10	90.488	75.5	67.85015923	8
temperate broadleaf evergreen tree	10	34.017	27	28.2627804	25
tropical broadleaf deciduous tree	10	129	129	41.01219331	2
temperate broadleaf deciduous tree	10	72.637	41.66	83.52495039	22
boreal broadleaf deciduous tree	10	50	50	NA	1
broadleaf evergreen shrub	10	65.353	29	116.0616668	16
broadleaf deciduous shrub	10	129.644	60	145.5387501	9
c3 grass	10	157.988	161	67.31744598	24
C4 grass	40	93.933	48.5	125.5325881	6
crop	10	60.629	36.7	60.74543722	21
					150

*New Value, Standard Deviation and n are based on data pooled from the literature.

Table 2. Global values from CLM simulations and observations[a]

Simulation	**$g_{s,n}$ data used**	**GPP (Pg C yr^{-1})**	**ET (10^3 km^3 yr^{-1})**	**Runoff (10^3 km^3 yr^{-1})**
Control	N/A	157.83	65.6148	30.462
g_o	Mean	152.56	72.6555	24.2141
g_{night}	Mean	156.068	66.0926	30.0724
g_{min}	Mean	151.252	68.6843	27.8161
g_o	Median	153.641	71.5441	25.1739
g_{night}	Median	156.346	66.031	30.119
g_{min}	Median	152.385	67.8881	28.51
Observation		119-175	65.13	37.7521

[a]Global gross primary productivity (GPP), evapotranspiration (ET) and runoff values. Observed values presented in Bonan et al. (2011), Welp et al. (2011), and Lawrence et al. (2011)

443

444

Figure Captions

Figure 1. Diurnal time-series of canopy conductance (a,c) and transpiration (b,d) for Ethiopia over five days in mid-January (a-b) and mid-July (c-d). The control simulation (solid black line) had lower conductance and transpiration than the Δg_o simulation (dotted red line) and the Δg_{min} simulation (dashed blue line). The Δg_{night} simulation (dot-dashed teal line) had higher nighttime conductance and transpiration than the control simulation, but similar daytime conductance and transpiration, allowing for daytime conductance to fall below the nighttime threshold. The Δg_o simulation added the observed $g_{s,n}$ values to the conductance calculation at every time, day or night, which is not theoretically aligned with the function of including observed $g_{s,n}$. As a result, the Δg_o simulation was eliminated from further analyses. Note that all minimum thresholds (g_o, g_{night}, and g_{min}) were adjusted using a soil moisture scalar.

Figure 2. Simulated average transpiration (a), runoff (d), and soil moisture (g) for a control simulation; and percent change from control in transpiration (b-c), runoff (e-f), and soil moisture (h-i) after including a nighttime threshold (Δg_{night}; b,e,h) or a minimum g_s threshold (Δg_{min}; c,f,i) based on observational data. Note that both nighttime and minimum thresholds were adjusted based on a soil moisture scalar.

Figure 3. Average gross primary productivity (GPP) for a control simulation (a), and percent change from control (b-c) after including a nighttime threshold (Δg_{night}; b) or a minimum g_s threshold (Δg_{min}; c) based on observational data.

Note that both nighttime and minimum thresholds were adjusted based on a soil moisture scalar.

Figure 4. Terrestrial coupling for June-July-August for a control simulation (a), and the difference from control (b-c) after including a nighttime threshold (Δg_{night}; b) or a minimum g_s threshold value (Δg_{min}; c) based on observational data. Note that both nighttime and minimum thresholds were adjusted based on a soil moisture scalar.

Figure 5. Average diel canopy transpiration for the months of May, June, and July in Castlereagh, Australia (observation, dotted black line), estimated from sap flux measurements of Red Gum and Iron Bark, the dominant tree species in the canopy. Average simulated canopy transpiration for the grid cell corresponding to Castlereagh, Australia for the control (unmodified; solid black line), Δg_o (Ball-Berry g_o parameter adjusted; red line), Δg_{night} (minimum nighttime threshold added; teal line), and Δg_{min} (minimum conductance threshold added; blue line) simulations. Error bars corresponding to the observations (dashed) and each simulation (solid) are colored accordingly, and are calculated as +/- one standard deviation from the mean. Note that the simulations use meteorological forcings from an atmospheric dataset (see Methods), not the local meteorology from when the measurements were collected (some meteorological data was collected at the site, but not all variables required by the model). The simulated grid cell covers a much larger area than the observational data collection site.

References

Ball, J. T.: An Analysis of Stomatal Conductance, Stanford University., 1988.

Ball, J. T., Woodrow, I. E. and Berry, J. A.: A Model Predicting Stomatal Conductance and its Contribution to the Control of Photosynthesis under Different Environmental Conditions, in Progress in Photosynthesis Research, edited by J. Biggins, pp. 221–224, Springer Netherlands. [online] Available from: http://link.springer.com/chapter/10.1007/978-94-017-0519-6_48 (Accessed 27 April 2015), 1987.

Barnard, D. M. and Bauerle, W. L.: The implications of minimum stomatal conductance on modeling water flux in forest canopies, J. Geophys. Res.-Biogeosciences, 118(3), 1322–1333, doi:10.1002/jgrg.20112, 2013.

Bonan, G. B., Lawrence, P. J., Oleson, K. W., Levis, S., Jung, M., Reichstein, M., Lawrence, D. M. and Swenson, S. C.: Improving canopy processes in the Community Land Model version 4 (CLM4) using global flux fields empirically inferred from FLUXNET data, J. Geophys. Res.-Biogeosciences, 116, G02014, doi:10.1029/2010JG001593, 2011.

Bonan, G. B., Oleson, K. W., Fisher, R. A., Lasslop, G. and Reichstein, M.: Reconciling leaf physiological traits and canopy flux data: Use of the TRY and FLUXNET databases in the Community Land Model version 4, J. Geophys. Res.-Biogeosciences, 117, G02026, doi:10.1029/2011JG001913, 2012.

Bonan, G. B., Williams, M., Fisher, R. A. and Oleson, K. W.: Modeling stomatal conductance in the earth system: linking leaf water-use efficiency and water transport along the soil–plant–atmosphere continuum, Geosci Model Dev, 7(5), 2193–2222, doi:10.5194/gmd-7-2193-2014, 2014.

Bowden, J. D. and Bauerle, W. L.: Measuring and modeling the variation in species-specific transpiration in temperate deciduous hardwoods, Tree Physiol., 28(11), 1675–1683, 2008.

Caird, M. A., Richards, J. H. and Donovan, L. A.: Nighttime stomatal conductance and transpiration in C-3 and C-4 plants, Plant Physiol., 143(1), 4–10, doi:10.1104/pp.106.092940, 2007.

Collatz, G. J., Ball, J. T., Grivet, C. and Berry, J. A.: Physiological and environmental regulation of stomatal conductance, photosynthesis and transpiration: a model that includes a laminar boundary layer, Agric. For. Meteorol., 54(2–4), 107–136, doi:10.1016/0168-1923(91)90002-8, 1991.

Dios, V. R. de, Turnbull, M. H., Barbour, M. M., Ontedhu, J., Ghannoum, O. and Tissue, D. T.: Soil phosphorous and endogenous rhythms exert a larger impact than CO2 or temperature on nocturnal stomatal conductance in Eucalyptus tereticornis, Tree Physiol., tpt091, doi:10.1093/treephys/tpt091, 2013.

Dirmeyer, P. A.: The terrestrial segment of soil moisture-climate coupling, Geophys. Res. Lett., 38, L16702, doi:10.1029/2011GL048268, 2011.

Fisher, J. B., Baldocchi, D. D., Misson, L., Dawson, T. E. and Goldstein, A. H.: What the towers don't see at night: nocturnal sap flow in trees and shrubs at two AmeriFlux sites in California, Tree Physiol., 27(4), 597–610, 2007.

Van Gorsel, E., Leuning, R., Cleugh, H. A., Keith, H., Kirschbaum, M. U. F. and Suni, T.: Application of an alternative method to derive reliable estimates of nighttime respiration from eddy covariance measurements in moderately complex topography, Agric. For. Meteorol., 148(6-7), 1174–1180, doi:10.1016/j.agrformet.2008.01.015, 2008.

Hetherington, A. M. and Woodward, F. I.: The role of stomata in sensing and driving environmental change, Nature, 424(6951), 901–908, doi:10.1038/nature01843, 2003.

Hirschi, M., Seneviratne, S. I., Alexandrov, V., Boberg, F., Boroneant, C., Christensen, O. B., Formayer, H., Orlowsky, B. and Stepanek, P.: Observational evidence for soil-moisture impact on hot extremes in southeastern Europe, Nat. Geosci., 4(1), 17–21, doi:10.1038/NGEO1032, 2011.

Kattge, J. and Knorr, W.: Temperature acclimation in a biochemical model of photosynthesis: a reanalysis of data from 36 species, Plant Cell Environ., 30(9), 1176–1190, doi:10.1111/j.1365-3040.2007.01690.x, 2007.

De Kauwe, M. G., Kala, J., Lin, Y.-S., Pitman, A. J., Medlyn, B. E., Duursma, R. A., Abramowitz, G., Wang, Y.-P. and Miralles, D. G.: A test of an optimal stomatal conductance scheme within the CABLE land surface model, Geosci Model Dev, 8(2), 431–452, doi:10.5194/gmd-8-431-2015, 2015.

Kirschbaum, M. U. F., Keith, H., Leuning, R., Cleugh, H. A., Jacobsen, K. L., van Gorsel, E. and Raison, R. J.: Modelling net ecosystem carbon and water exchange of a temperate Eucalyptus delegatensis forest using multiple constraints, Agric. For. Meteorol., 145(1-2), 48–68, doi:10.1016/j.agrformet.2007.04.002, 2007.

Lawrence, D. M., Oleson, K. W., Flanner, M. G., Thornton, P. E., Swenson, S. C., Lawrence, P. J., Zeng, X., Yang, Z.-L., Levis, S., Sakaguchi, K., Bonan, G. B. and Slater, A. G.: Parameterization Improvements and Functional and Structural Advances in Version 4 of the Community Land Model, J. Adv. Model. Earth Syst., 3, M03001, doi:10.1029/2011MS000045, 2011.

Leuning, R.: A critical appraisal of a combined stomatal-photosynthesis model for C3 plants, Plant Cell Environ., 18(4), 339–355, doi:10.1111/j.1365-3040.1995.tb00370.x, 1995.

Li, H., Huang, M., Wigmosta, M. S., Ke, Y., Coleman, A. M., Leung, L. R., Wang, A. and Ricciuto, D. M.: Evaluating runoff simulations from the Community Land Model 4.0 using observations from flux towers and a mountainous watershed, J. Geophys. Res.-Atmospheres, 116, D24120, doi:10.1029/2011JD016276, 2011.

McLaughlin, S. B., Wullschleger, S. D., Sun, G. and Nosal, M.: Interactive effects of ozone and climate on water use, soil moisture content and streamflow in a

572 southern Appalachian forest in the USA, New Phytol., 174(1), 125–136,
573 doi:10.1111/j.1469-8137.2007.01970.x, 2007.

574 Medlyn, B. E., Robinson, A. P., Clement, R. and McMurtrie, R. E.: On the validation
575 of models of forest CO2 exchange using eddy covariance data: some perils and
576 pitfalls, Tree Physiol., 25(7), 839–857, 2005.

577 Medlyn, B. E., Duursma, R. A., Eamus, D., Ellsworth, D. S., Prentice, I. C., Barton, C.
578 V. M., Crous, K. Y., De Angelis, P., Freeman, M. and Wingate, L.: Reconciling the
579 optimal and empirical approaches to modelling stomatal conductance, Glob.
580 Change Biol., 17(6), 2134–2144, doi:10.1111/j.1365-2486.2010.02375.x, 2011.

581 Miralles, D. G., Teuling, A. J., van Heerwaarden, C. C. and Vilà-Guerau de Arellano,
582 J.: Mega-heatwave temperatures due to combined soil desiccation and
583 atmospheric heat accumulation, Nat. Geosci., 7(5), 345–349,
584 doi:10.1038/ngeo2141, 2014.

585 Niyogi, D. S. and Raman, S.: Comparison of Four Different Stomatal Resistance
586 Schemes Using FIFE Observations, J. Appl. Meteorol., 36(7), 903–917,
587 doi:10.1175/1520-0450(1997)036<0903:COFDSR>2.0.CO;2, 1997.

588 Oleson, K. W., Lawrence, D. M., Bonan, G. B., Drewniak, B., Huang, M., Koven, C. D.,
589 Levis, S., Li, F., Riley, W. J., Subin, Z. M., Swenson, S. C., Thornton, P. E., Bozbiyik,
590 A., Fisher, R. A., Kluzek, E., Lamarque, J.-F., Lawrence, P. J., Leung, L. R., Lipscomb,
591 W., Muszala, S., Ricciuto, D. M., Sacks, W. J., Sun, Y., Tang, J. Y. and Yang, Z.-L.:
592 Technical Description of version 4.5 of the Community Land Model (CLM), NCAR
593 Tech. Note, NCAR/TN-503+STR, doi:10.5065/D6RR1W7M, 2013.

594 Phillips, N. G., Lewis, J. D., Logan, B. A. and Tissue, D. T.: Inter- and intra-specific
595 variation in nocturnal water transport in Eucalyptus, Tree Physiol., 30(5), 586–
596 596, doi:10.1093/treephys/tpq009, 2010.

597 Scholz, F. G., Bucci, S. J., Goldstein, G., Meinzer, F. C., Franco, A. C. and Miralles-
598 Wilhelm, F.: Removal of nutrient limitations by long-term fertilization decreases
599 nocturnal water loss in savanna trees, Tree Physiol., 27(4), 551–559,
600 doi:10.1093/treephys/27.4.551, 2007.

601 Sellers, P. j., Randall, D. a., Collatz, G. j., Berry, J. a., Field, C. b., Dazlich, D. a., Zhang,
602 C., Collelo, G. d. and Bounoua, L.: A Revised Land Surface Parameterization (SiB2)
603 for Atmospheric GCMS. Part I: Model Formulation, J. Clim., 9(4), 676–705,
604 doi:10.1175/1520-0442(1996)009<0676:ARLSPF>2.0.CO;2, 1996.

605 Wei, J. and Dirmeyer, P. A.: Dissecting soil moisture-precipitation coupling,
606 Geophys. Res. Lett., 39, L19711, doi:10.1029/2012GL053038, 2012.

607 Zeppel, M. J. B., Lewis, J. D., Phillips, N. G. and Tissue, D. T.: Consequences of
608 nocturnal water loss: a synthesis of regulating factors and implications for
609 capacitance, embolism and use in models, Tree Physiol., 34(10), 1047–1055,
610 doi:10.1093/treephys/tpu089, 2014.

611

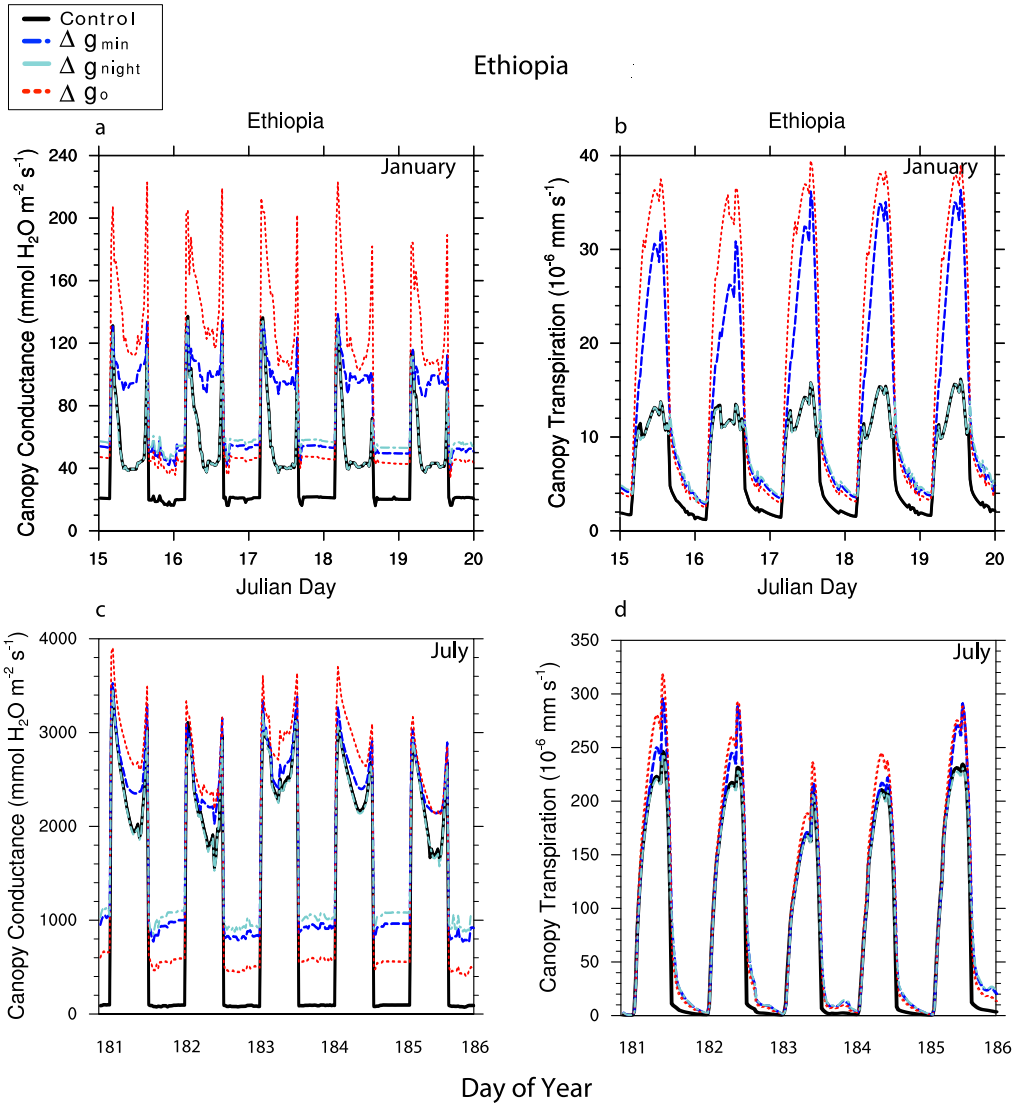
Control
Δ g min
Δ g night
Δ go
Ethiopia
a
Ethiopia
January
Canopy Conductance (mmol H2O m-2 s-1)
Julian Day
b
Ethiopia
January
Canopy Transpiration (10-6 mm s-1)
Julian Day
c
July
Canopy Conductance (mmol H2O m-2 s-1)
d
July
Canopy Transpiration (10-6 mm s-1)
Day of Year

612
613

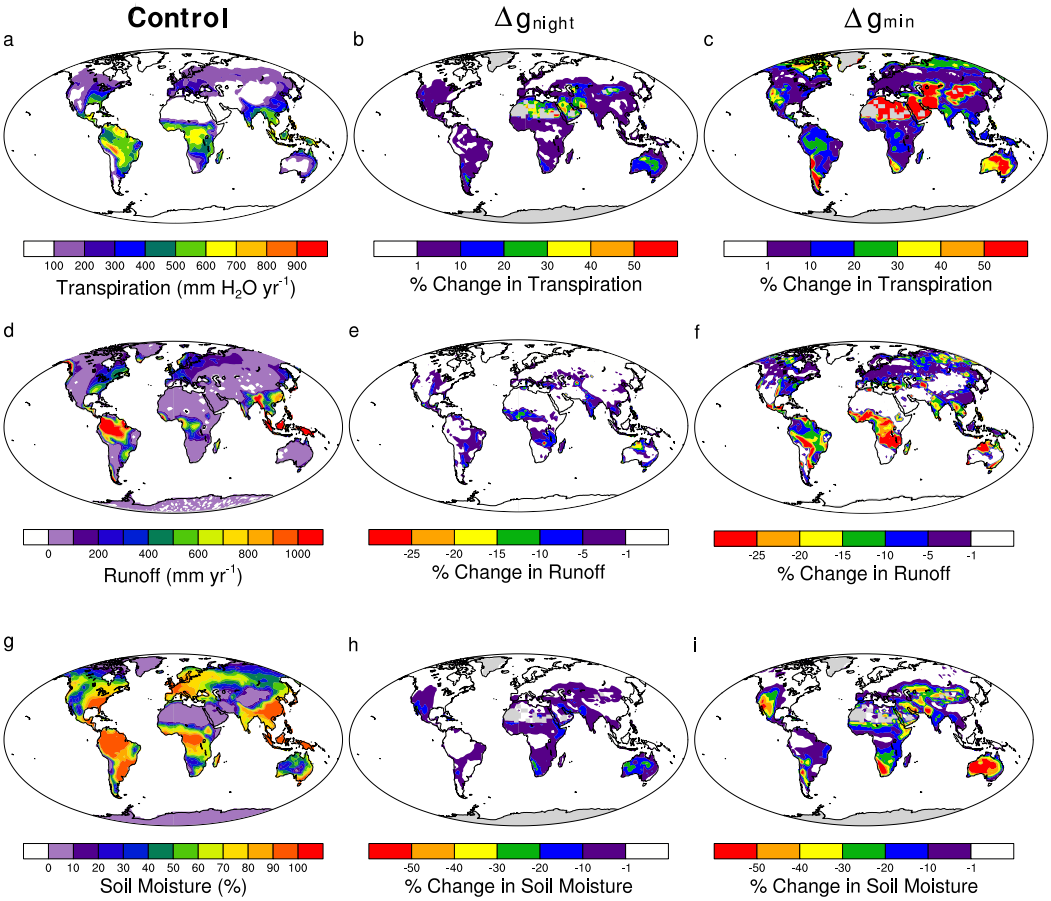
Control
Δgnight
Δgmin
a
b
c
100 200 300 400 500 600 700 800 900
Transpiration (mm H2O yr-1)
1 10 20 30 40 50
% Change in Transpiration
1 10 20 30 40 50
% Change in Transpiration
d
e
f
0 200 400 600 800 1000
Runoff (mm yr-1)
-25 -20 -15 -10 -5 -1
% Change in Runoff
-25 -20 -15 -10 -5 -1
% Change in Runoff
g
h
i
0 10 20 30 40 50 60 70 80 90 100
Soil Moisture (%)
-50 -40 -30 -20 -10 -1
% Change in Soil Moisture
-50 -40 -30 -20 -10 -1
% Change in Soil Moisture

614

615

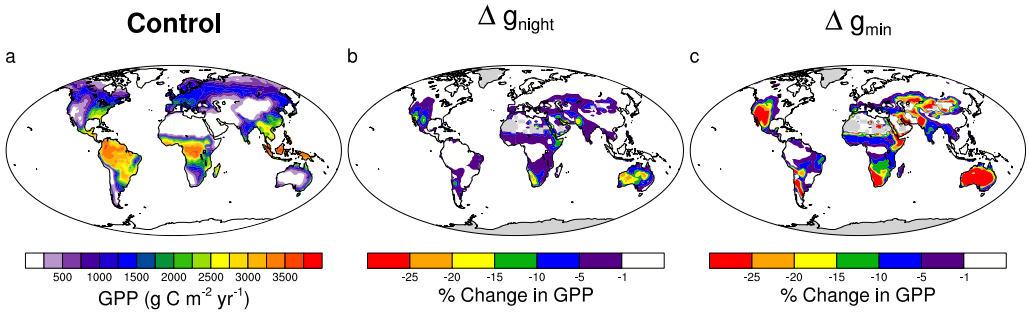
Control
Δ g night
Δ g min
a
b
c
500 1000 1500 2000 2500 3000 3500
GPP (g C m-2 yr-1)
-25 -20 -15 -10 -5 -1
% Change in GPP
-25 -20 -15 -10 -5 -1
% Change in GPP

616

617

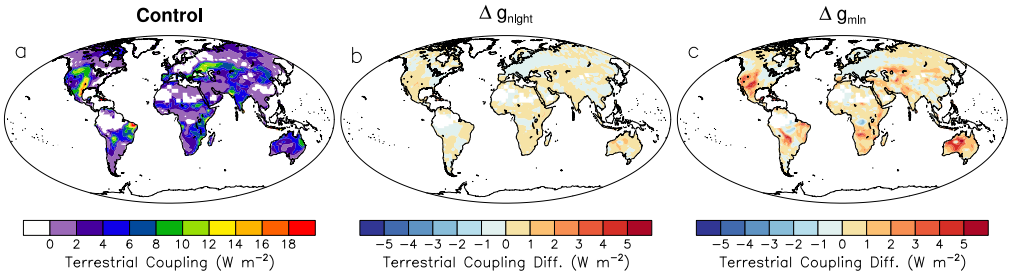
Control
a
Δ g_nlght
b
Δ g_mln
c
0 2 4 6 8 10 12 14 16 18
Terrestrial Coupling (W m⁻²)
−5 −4 −3 −2 −1 0 1 2 3 4 5
Terrestrial Coupling Diff. (W m⁻²)
−5 −4 −3 −2 −1 0 1 2 3 4 5
Terrestrial Coupling Diff. (W m⁻²)

618

619

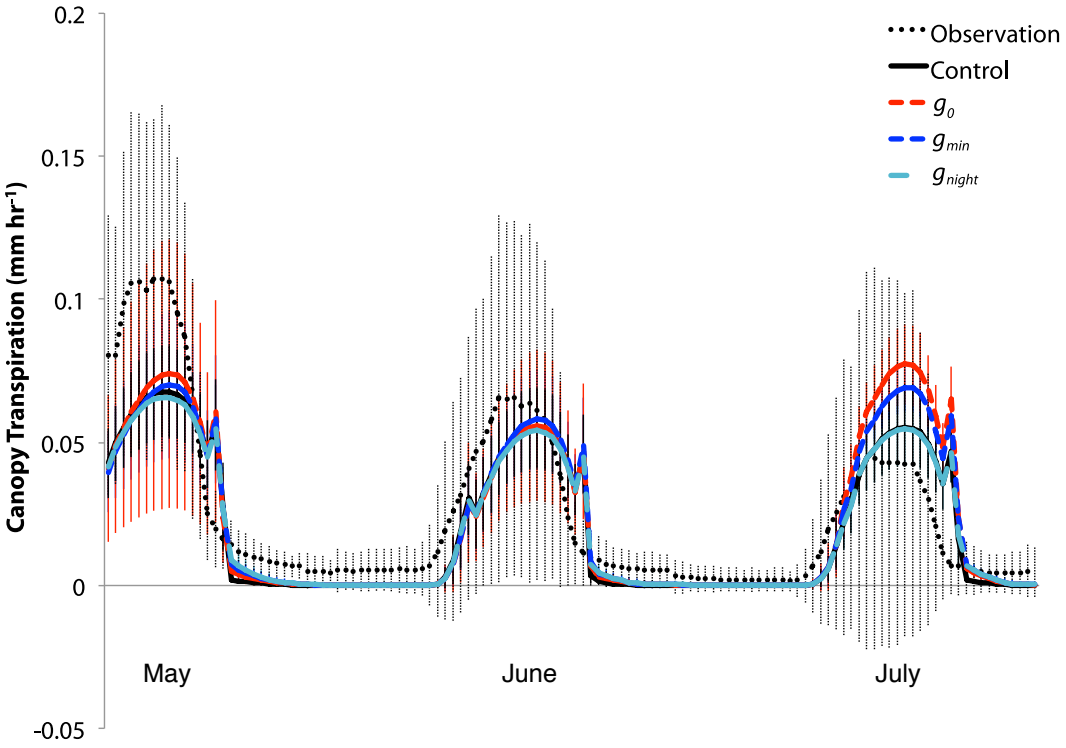
0.2
0.15
0.1
0.05
0
-0.05
Canopy Transpiration (mm hr-1)
May
June
July
Observation
Control
g0
gmin
gnight

620